PROCEEDINGS OF SCIENCE

K- and $D_{(s)}$-meson leptonic decay constants with physical light, strange and charm quarks by ETMC

P. Dimopoulos,[a,*] **R. Frezzotti,**[b] **M. Garofalo**[c] **and S. Simula**[d]

[a] *Dipartimento di Scienze Matematiche, Fisiche e Informatiche, Università di Parma, Parma, Italy*
[b] *Dipartimento di Fisica and INFN, Università di Roma "Tor Vergata", I-00133 Rome, Italy*
[c] *HISKP (Theory), Rheinische Friedrich-Wilhelms-Universität Bonn, Germany*
[d] *Istituto Nazionale di Fisica Nucleare, Sezione di Roma Tre, Italy*

E-mail: petros.dimopoulosATunipr.it

We present a lattice QCD computation and preliminary results for the leptonic decay constants of the pseudoscalar mesons K, D and D_s in the isosymmetric QCD limit. The computation is based on simulations of $N_f = 2 + 1 + 1$ dynamical quarks performed by the Extended Twisted Mass Collaboration (ETMC), where the light, strange and charm quark masses are all tuned at their physical values. We also present preliminary unitarity checks for the first and second rows of the Cabibbo-Kobayashi-Maskawa matrix.

The 38th International Symposium on Lattice Field Theory, LATTICE2021 26th-30th July, 2021 Zoom/Gather@Massachusetts Institute of Technology

*Speaker

PoS(LATTICE2021)472

1. Introduction

Of the most important hadronic inputs for obtaining estimates of the Cabibbo-Kobayashi-Maskawa (CKM) matrix elements (ME) are the values of the leptonic decay constants of pseudoscalar (PS) mesons. In these proceedings we present a high precision lattice QCD (LQCD) calculation for the K, D and D_s PS-meson decay constants using $N_f = 2+1+1$ gauge ensembles generated by the Extended Twisted Mass Collaboration (ETMC).

2. Lattice action and simulations

We employ the twisted mass (tm) fermionic formulation that ensures automatic O(a)-improvement for all observables as far as tuning at maximal twist is in place Refs [1, 2]. Moreover as it has been shown in Refs [3–6] the inclusion of the clover term in the maximally twisted fermionic action provides the beneficial property of reduced O(a^2) cutoff and isospin breaking effects.

ETMC has performed $N_f = 2+1+1$ dynamical quark simulations employing the sea quark action written as $S_{sea} = S_g^{\rm Iwa} + S_{tm}^{\ell} + S_{tm}^{h}$, where $S_g^{\rm Iwa}$ is the Iwasaki improved gauge action [7] and

$$S_{tm}^{\ell} = \sum_x \bar{\chi}_\ell(x)\left[D_W(U) + \frac{i}{4}c_{\rm SW}\sigma^{\mu\nu}\mathcal{F}^{\mu\nu}(U) + m_{0\ell} + i\mu_\ell\tau^3\gamma^5\right]\chi_\ell(x)\,, \tag{1}$$

$$S_{tm}^{h} = \sum_x \bar{\chi}_h(x)\left[D_W(U) + \frac{i}{4}c_{\rm SW}\sigma^{\mu\nu}\mathcal{F}^{\mu\nu}(U) + m_{0h} - \mu_\delta\tau_1 + i\mu_\sigma\tau^3\gamma^5\right]\chi_h(x)\,, \tag{2}$$

are, respectively, the fermionic actions used in the light (S_{tm}^{ℓ}) and strange-charm (S_{tm}^{h}) quark sectors. Notice that in Eq. (1) $\chi_\ell = (u,d)^T$ represents the light quark doublet, while the degenerate light twisted and the (untwisted) Wilson quark masses are denoted by μ_ℓ and $m_{0\ell}$, respectively. For the heavy quark action, Eq. (2), the doublet $\chi_h = (s,c)^T$ represents the mass non-degenerate strange and charm quarks. Here m_{0h} denotes the (untwisted) Wilson quark mass while the parameters μ_δ and μ_σ in combination with the presence of the Pauli matrices τ_1 and τ_3 lead to quark mass non-degeneracy, see Ref. [2]. In both equations $D_W(U)$ is the massless Wilson-Dirac operator, and the Sheikoleslami-Wohlert improvement term, $c_{\rm SW}\sigma^{\mu\nu}\mathcal{F}^{\mu\nu}(U)$, has been included for the reason already explained above. The value for the clover parameter $c_{\rm SW}$ is set by using the 1–loop tadpole boosted estimate as presented in Ref. [8]. The condition of maximal twist is achieved by tuning the hopping parameter κ for the untwisted Wilson quark mass such as $m_{0\ell} = m_{0h} = m_{crit}$. Details about the lattice action and the algorithmic setup are presented in Refs [3, 9, 10].

Simulations have been carried out reaching the physical mass values of both light and heavy (strange and charm) quarks. As for the latter the sea quark mass parameters (μ_σ and μ_δ) have been tuned so that the two phenomenological conditions $m_c/m_s = 11.8$ and $m_{D_s}/f_{D_s} = 7.9$ [11] are accurately reproduced by each of the $N_f = 2+1+1$ ensembles.

In order to avoid O(a^2) mixing effects in the physical observables involving the heavy quarks (strange and charm), owing to the form of the sea quark action of Eq. (2), we opted for a non-unitary lattice setup. Therefore in the valence sector we employ the Osterwalder-Seiler fermionic regularisation [12] which treats the strange and charm quarks in a flavour diagonal way. The valence action in the strange and charm sectors is given by:

$$S_{val}^{f} = \sum_{x} \bar{\chi}_{f}^{val}(x) \left(D_{W}^{cr}(U) + \frac{i}{4} c_{SW} \sigma^{\mu\nu} \mathcal{F}^{\mu\nu}(U) + i\gamma_5 \mu_f \right) \chi_{f}^{val}(x) \ , f = s, c, \tag{3}$$

where $D_{W}^{cr}(U) \equiv D_W(U)|_{m_0 = m_{crit}}$ is the critical Wilson-Dirac operator and χ_f^{val} denotes single quark flavour field. It has been shown in Ref. [13] that this kind of mixed action preserves the automatic O(a)-improvement of physical observables, i.e. lattice artifacts, including those violating unitarity, scale as O(a^2) implying that unitarity is safely recovered in the continuum limit.

In this study we use $N_f = 2 + 1 + 1$ simulations performed at three values of the lattice spacing in the range $[0.69, 0.95]$ fm and at several pseudoscalar mass values spanning from the physical pion mass up to 350 MeV. In Table 1 essential simulation details are presented. For the computation of w_0/a and the gradient-flow w_0-determination, we refer the reader to Refs [9, 14, 15]. The scale setting is performed using the isosymmetric QCD value $f_{\pi}^{isoQCD} = 130.4(2)$ [16].

The present lattice computation is performed in the isoymmetric QCD limit. However future work based on the same gauge ensembles is planned in order to take into account isospin breaking effects along the lines of the work of *e.g.* Ref [17].

β	Ens.	(L, T)	M_π (MeV)	# meas.	w_0/a
1.726	cA211.12.48	(48,96)	167	322	1.8355(35)
	cA211.30.32	(32,64)	261	1237	
	cA211.40.24	(24,48)	302	662	
	cA211.53.24	(24,48)	346	628	
1.778	cB211.072.64	(64,128)	137	374	2.1300(16)
	cB211.14.64	(64,128)	190	437	
	cB211.25.48	(48,96)	253	314	
	cB211.25.32	(32,64)	253	400	
1.836	cC211.06.80	(80,160)	134	401	2.5045(17)
	cC211.20.48	(48,96)	246	890	

Table 1: Simulation details for the $N_f = 2 + 1 + 1$ ensembles by ETMC.

3. Determination of pseudoscalar meson decay constants with tmQCD

In the maximal tm (Mtm) formulation of LQCD the computation of pseudoscalar decay constants does not require any (re)normalisation constant thanks to the existence of a conserved current [1, 18]. It is thus sufficient to employ correlation functions of the type $C_{PP}(t) = (1/L^3) \sum_{\vec{x},\vec{y}} \langle 0| P_{ff'}(\vec{x}, t) P_{ff'}^{\dagger}(\vec{y}, 0)|0\rangle$, where $P_{ff'}(x) = \bar{\chi}_f^{val}(x)\gamma_5 \chi_{f'}^{val}(x)$ (with flavours $\{f, f'\} = \{\ell, s, c\}$) is the pseudoscalar density operator. Then the leptonic decay constant of a PS-meson with mass denoted by $M_{ps(ff')}$ made out of valence quark flavours with bare masses μ_f and $\mu_{f'}$ is given by

$$f_{ps} = (\mu_f + \mu_{f'}) \frac{\langle 0|P_{ff'}|ps\rangle}{M_{ps(ff')} \sinh(M_{ps(ff')})} \ , \tag{4}$$

which is automatically O(a)-improved owing to the maximal twist condition ($m_0^{val} = m_{0\ell} = m_{0h} = m_{crit}$).

In the present computation we make use of the quark mass results for the u/d, s and c presented in Section V of Ref. [14] and corresponding to the meson sector analysis. In this way we can employ the same mesonic correlation functions as in Ref. [14] and hence determine correctly the error propagation owing to the quark masses' uncertainties. We recall that in the framework of Mtm LQCD the renormalised quark mass of a quark flavour f is given by $m_f = \mu_f / Z_P$, where Z_P is the renormalization constant for the pseudoscalar density operator, the determination of which has been presented in Refs [14, 19].

For the statistical and fit error analysis we have employed the jackknife method. We have determined the continuum limit values at the physical light quark mass u/d by making use of simultaneous continuum and chiral fits. For the estimation of the various sources of systematic uncertainty we repeat our analysis by employing different kinds of fit ansätze regarding the chiral extrapolation/interpolation to the physical light quark mass u/d. Furthermore we perform several analyses by using data combinations corresponding to two out of three lattice spacings and also by employing different determinations for Z_P that differ by $\mathrm{O}(a^2)$ effects. For a given decay constant we thus obtain a distribution of results, with each result corresponding to a different analysis and a total number of analyses ranging from 32 to 96 (depending on the considered decay constant). From such a distribution the mean value and the uncertainty of the final result are estimated using the combination method and formulae discussed in Sec. V of Ref. [14] (see there Eqs (38)–(43)).

4. Determinations of f_K and f_K/f_π

In the determination of f_K we first interpolate the decay constant estimates to the strange quark mass and then we employ simultaneous continuum and chiral fits of the quantity $f_{s\ell}$ against the light quark mass m_ℓ. We make use of two fit ansätze, namely the next-to-leading order (NLO) SU(2) ChPT formula, $f_{s\ell} = P_0\,(1-(3/4)\xi_\ell \log \xi_\ell + P_1 \xi_\ell + P_2 a^2)\,\mathrm{K}^{\mathrm{FSE}}_{f_K}$ and a polynomial quadratic fit of the form $f_{s\ell} = Q'_0 \left(1 + Q'_1 m_\ell + Q'_2 m_\ell^2 + Q'_3 a^2\right) \mathrm{K}^{\mathrm{FSE}}_{f_K}$. In the first one it is set $\xi_\ell = (2B_0 m_\ell)/(4\pi f_0)^2$ where B_0 and f are the SU(2) ChPT low-energy constants (LECs) obtained from the quark mass analysis, see Ref [14]. The factor $\mathrm{K}^{\mathrm{FSE}}_{f_K}$ represents the estimation for the (small) correction to our data due to finite size volume effects (FSE) following [20].

We work in a similar way for the determination of the ratio f_K/f_π for which we make use of the following two fit ansätze: $f_{s\ell}/f_{\ell\ell} = P'_0\,(1 + (5/4)\xi_\ell \log \xi_\ell + P'_1 \xi_\ell + P'_2 a^2)\,\mathrm{K}^{\mathrm{FSE}}_{f_K/f_\pi}$ and $f_{s\ell}/f_{\ell\ell} = Q'_0 \left(1 + Q'_1 m_\ell + Q'_2 m_\ell^2 + Q'_3 a^2\right) \mathrm{K}^{\mathrm{FSE}}_{f_K/f_\pi}$. In Fig. 1 we show a representative plot out of several analyses concerning the simultaneous chiral and continuum fits for f_K (left panel) and f_K/f_π (right panel). In both cases the (NLO) SU(2) ChPT and polynomial fits to our data are of good quality and the corresponding continuum results at the physical point are compatible. After averaging over results from all available analyses our *preliminary* results and the respective error budgets for the two quantities are

$$f_K^{\mathrm{isoQCD}} = 155.3(0.9)_{\mathrm{(stat+fit)}}(0.1)_{Z_P}(0.2)_{\mathrm{chiral}}(1.4)_{\mathrm{discr.}}(0.2)_{\mathrm{FSE}}\;[1.7]\ \mathrm{MeV} \tag{5}$$

$$(f_K/f_\pi)^{\mathrm{isoQCD}} = 1.2023(38)_{\mathrm{(stat+fit)}}(3)_{Z_P}(11)_{\mathrm{chiral}}(8)_{\mathrm{discr.}}(5)_{\mathrm{FSE}}\;[41], \tag{6}$$

where separate errors in parentheses are due to the indicated sources of uncertainty while the total error is shown in brackets. Notice that the estimate for $(f_K/f_\pi)^{\mathrm{isoQCD}}$ has a total uncertainty of about

0.34% and it shows nice agreement with the result of Ref. [9], namely $(f_K/f_\pi)^{\rm isoQCD} = 1.1995\,(44)$, where an analysis of the same data has been performed but in terms of the PS-meson masses. Note also that a much more precise estimate for the K-decay constant, still in good agreement with the result of Eq. (5), is obtained by

$$f_K^{\rm isoQCD} = (f_K/f_\pi)^{\rm isoQCD} \times f_\pi^{\rm (isoQCD)} = 156.8(0.6)\ {\rm MeV}.$$

Finally, by employing the estimate of the strong isospin effects correction computed in Ref. [17] (in the GRS scheme [21]) we also obtain:

$$f_{K^\pm}/f_{\pi^\pm} = 1.1984\,(41) \ \text{ and } \ f_{K^\pm} = (f_{K^\pm}/f_{\pi^\pm}) \times f_\pi^{\rm (phys.)} = 156.3(0.6)\ {\rm MeV}$$

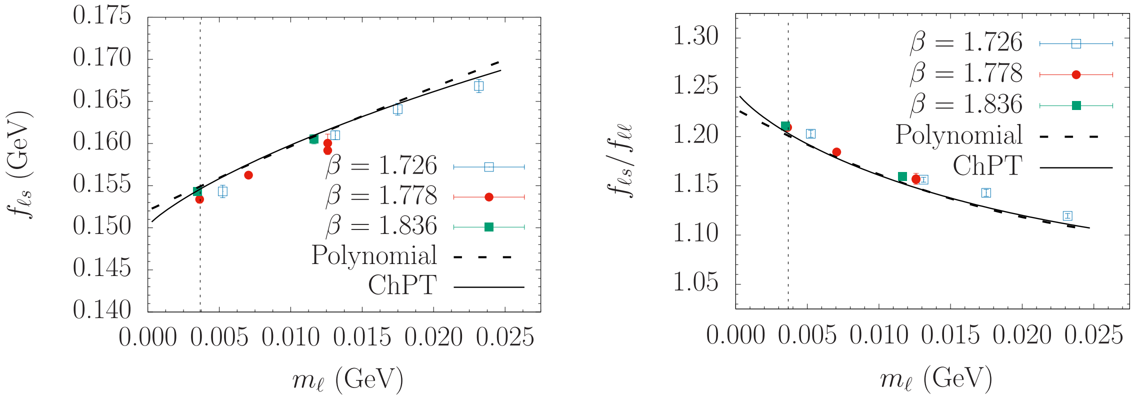

Figure 1: Plots showing simultaneous chiral and continuum fits (continuum limit curves are shown) for f_K (left) and f_K/f_π (right) against the renormalised light quark mass $m_\ell(\overline{\rm MS}, 2\ {\rm GeV})$. Ansätze for chiral and polynomial fits are given in the text. In both plots the vertical dotted line indicates the physical value of $m_{u/d}$.

5. Determinations of f_{D_s}, f_D and f_{D_s}/f_D

We compute f_{D_s} by first interpolating the decay constant estimates to the strange and charm quark masses before we employ a combined chiral and continuum fit of the data for f_{sc} in terms of m_ℓ and a^2. We try two kinds of intermediate scaling variables that are the gradient flow w_0 and the pseudocalar mass M_{sc}, the latter computed at each value of m_ℓ. The fit ansatz for both scaling variable choices is of the form $f_{sc} = c_0\left(1 + c_1 m_\ell + c_3 a^2\right)$ that is linear in m_ℓ and it describes nicely our data as it can be appreciated by the two plots in Fig. 2. Dependence on m_ℓ, according to the expectations, is quite weak. It should be also added that the continuum limit results from both ways of analysis are in perfect agreement, nevertheless when M_{sc} is employed as the scaling variable cut off effects are clearly suppressed.

For the calculation of the ratio f_{D_s}/f_D we employ the following three fit ansätze, where the first two ansätze are polynomial fits (linear or quadratic) in m_ℓ, namely $f_{sc}/f_{\ell c} = \tilde{Q}_0(1 + \tilde{Q}_1 m_\ell + [\tilde{Q}_2 m_\ell^2] + \tilde{Q}_3 a^2)$, and the third one is based on the HMChPT prediction and takes the form $f_{sc}/f_{\ell c} = \tilde{P}_0(1 + \frac{3}{4}(1+3\hat{g}^2)\xi_\ell \log(\xi_\ell) + \tilde{P}_1 m_\ell + \tilde{P}_2 a^2)$, where $\hat{g} = 0.61(7)$ is obtained from the experimental measurement of the $g_{D^\star D\pi}$. In Fig. 3 we present a representative analysis plot for the

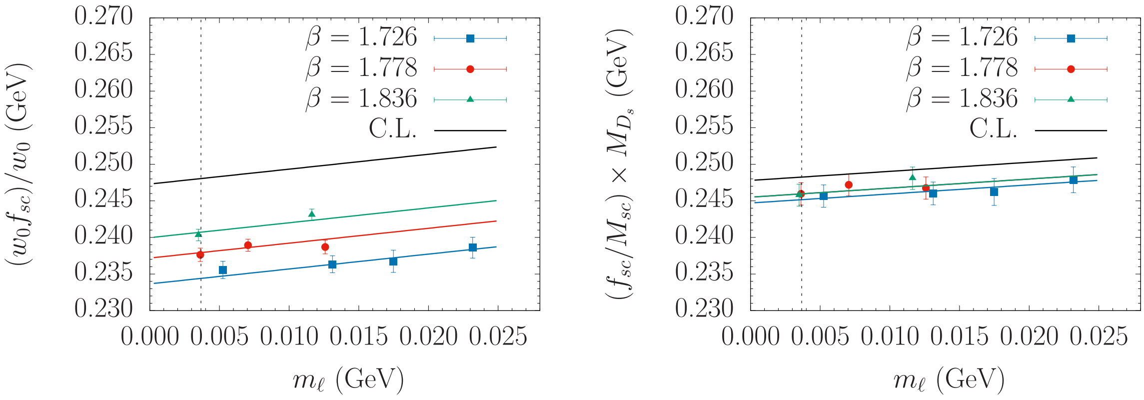

Figure 2: Plots showing simultaneous chiral and continuum fit for f_{D_s} in terms of intermediate scaling variable w_0 (left) and of a PS-meson mass M_{sc} (right) against the renormalised light quark mass $m_\ell(\overline{\text{MS}}, 2\text{ GeV})$. In both plots the vertical dotted line indicates the physical value of $m_{u/d}$ and "C.L." is for the continuum limit curve.

ratio f_{Ds}/f_D against m_ℓ where all three kinds of combined continnum and chiral fits are shown. We find that the HMCHPT fit describes rather poorly our data. Therefore having data at (or close to) the physical point we trust as for the central value and the error only fits of good quality which in the present case are the two kinds of the polynomial chiral fit ansatz. Finally, we can compute

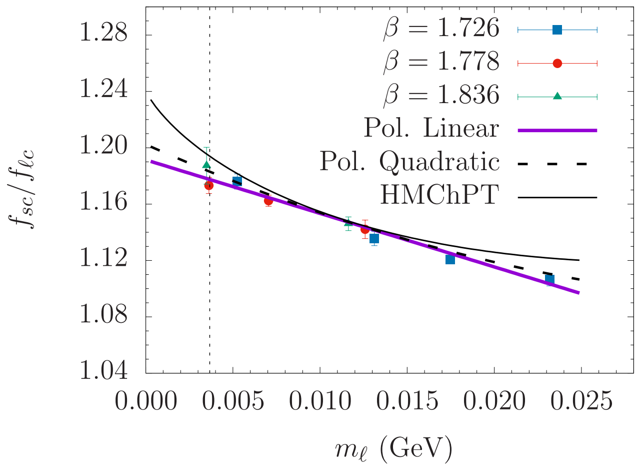

Figure 3: Simultaneous continuum and chiral fits (continuum limit curves are shown) for the ratio f_{D_s}/f_D against the renormalised light quark mass $m_\ell(\overline{\text{MS}}, 2\text{ GeV})$ using various chiral fit ansätze. Vertical dotted line indicates the physical value of $m_{u/d}$.

f_D directly and indirectly. In the first way, the direct one, we follow an analysis similar to the f_{Ds} case i.e. we employ two kinds of intermediate scaling variable. As for the chiral fit ansatz we employ both polynomial and HMChPT fits. We observe that, similarly to the f_{D_s} case, the use of a PS-meson mass of the type $M_{\ell c}$ playing the role of intermediate scaling variable leads to suppressed discretisation effects. Moreover as it happens for the analysis of the ratio f_{Ds}/f_D, also in the case of f_D the HMChPT fit ansatz does not provide a satisfactory fit quality. The indirect way for the

Quantity	**ETMC 21** ($N_f = 2+1+1$)	**ETMC 14** (N_f = 2+1+1)	**FLAG 19** (N_f = 2+1+1)	**FLAG 19** (N_f = 2+1)
$(f_K/f_\pi)^{\text{isoQCD}}$	1.2023(41)	1.188(15)	-	
$f_{K^\pm}/f_{\pi^\pm}$	1.1984(41)	1.184(16)	1.1932(19)	1.1917(37)
f_K^{isoQCD} (MeV)	155.3(1.7)	155.0(1.9)	-	-
$f_K^{\text{isoQCD}} = (f_K/f_\pi)^{\text{isoQCD}} \times f_\pi^{(\text{isoQCD})}$ (MeV)	156.8(0.6)	154.9(1.9)	-	-
$f_{K^\pm} = (f_{K^\pm}/f_{\pi^\pm}) \times f_\pi^{(\text{phys.})}$ (MeV)	156.3(0.6)	154.4(2.0)	155.7(0.3)	155.7(0.7)
f_{D_s} (MeV)	248.9(2.0)	247.2(4.1)	249.9(0.5)	248.0(1.6)
f_{D_s}/f_D	1.1838(115)	1.192(22)	1.1783(16)	1.1740(70)
f_D (MeV)	210.1(2.4)	207.4(3.8)	212.0(0.7)	209.0(2.4)
$(\frac{f_{D_s}}{f_D})/(\frac{f_K}{f_\pi})$	0.995(13)	1.003(14)	-	-

Table 2: Comparison of (*preliminary*) results for the PS-meson decay constants of the present work (ETMC 21) with previous ETMC results (ETMC 14 [22]) and FLAG 19 averages [11].

computation of f_D consists in combining our results for the ratio and the D_s decay constants as follows $f_D = f_{D_s}/(f_{D_s}/f_D)$.

Our *preliminary* results and error budget read:

$$f_{D_s} = 248.9\ (1.6)_{(\text{stat+fit})}(0.5)_{Z_P}(0.2)_{\text{chiral}}(1.0)_{\text{discr.}}\ [2.0]\ \text{MeV} \tag{7}$$

$$f_D = 210.1\ (2.2)_{(\text{stat+fit})}(0.1)_{Z_P}(0.4)_{\text{chiral}}(0.8)_{\text{discr.}}\ [2.4]\ \text{MeV} \tag{8}$$

$$f_{D_s}/f_D = 1.1838\ (90)_{(\text{stat+fit})}(25)_{Z_P}(38)_{\text{chiral}}(57)_{\text{discr.}}\ [115], \tag{9}$$

where the total error for each quantity is shown in brackets. Notice that the total relative errors for f_{Ds}, f_D and f_{D_s}/f_D are 0.8%, 1.1% and 1.0%, respectively.

6. Summary and results comparisons

In Table 2 we provide the comparison of the present work results (ETMC 21) with older ETMC results (ETMC 14 [22]), the latter obtained with $N_f = 2+1+1$ simulations but far from the physical point, and also with the FLAG 19 averages [11]. We would like to stress the higher precision of the ETMC 21 results with respect to the corresponding ETMC 14 ones owing to a remarkable reduction of both statistical and systematic uncertainties. We also notice that the ETMC 21 results compare well with the corresponding FLAG 19 averages.

Finally, by combining our results for the decay constants with the relevant experimental inputs we provide estimates for several of the first and second row elements of the CKM matrix. We get the following *preliminary* results: $|V_{us}/V_{ud}| = 0.2303(8)_{\text{th}}(3)_{\text{expt}}[8]$, $|V_{us}| = 0.2242(8)_{\text{th}}(3)_{\text{expt}}[8]$, $|V_{cd}| = 0.2199(25)_{\text{th}}(57)_{\text{expt}}[62]$ and $|V_{cs}| = 0.9871(79)_{\text{th}}(185)_{\text{expt}}[201]$. Thanks to the above estimates for the unitarity checks of the first and the second CKM rows we get:

$$|V_{ud}|^2 + |V_{us}|^2 + |V_{ub}|^2 - 1 = -1.56(0.34)_{\text{th}}(0.62)_{\text{expt}}[0.71] \times 10^{-3} \tag{10}$$

$$|V_{cd}|^2 + |V_{cs}|^2 + |V_{cb}|^2 - 1 = +2.3(1.6)_{\text{th}}(3.7)_{\text{expt}}[4.0] \times 10^{-2}. \tag{11}$$

where $|V_{ub}|^2$ and $|V_{cb}|^2$ being of order 10^{-6} and 10^{-4}, respectively, have negligible impact to the present accuracy. Our results lead to about 2σ tension for the unitarity check of the first row (at the per mille level) while they confirm the second row unitarity of the CKM matrix at the percent level.

Acknowledgments

We acknowledge PRACE (Partnership for Advanced Computing in Europe) for awarding us access to the high-performance computing system Marconi and Marconi100 at CINECA (Consorzio Interuniversitario per il Calcolo Automatico dell'Italia Nord-orientale) under the grants Pra17-4394, Pra20-5171 and Pra22-5171, and CINECA for providing us CPU time under the specific initiative INFN-LQCD123. The authors gratefully acknowledge the Gauss Centre for Supercomputing e.V. (www.gauss-centre.eu) for funding this project by providing computing time through the John von Neumann Institute for Computing (NIC) on the GCS Supercomputers Jureca and Jureca Booster [23] at Jülich Supercomputing Centre (JSC). P.D. acknowledges support form the European Unions Horizon 2020 research and innovation programme under the Marie Sklodowska-Curie grant agreement No. 813942 (EuroPLEx) and from INFN under the research project INFN-QCDLAT. R.F. acknowledges the University of Rome Tor Vergata for the support granted to the project PLNUGAMMA.

References

[1] R. Frezzotti and G.C. Rossi, *Chirally improving wilson fermions. i: O(a) improvement*, *JHEP* **08** (2004) 007 [hep-lat/0306014].

[2] R. Frezzotti and G.C. Rossi, *Twisted-mass lattice QCD with mass non-degenerate quarks*, *Nucl. Phys. Proc. Suppl.* **128** (2004) 193 [hep-lat/0311008].

[3] [ETMC] C. Alexandrou et al., *Simulating twisted mass fermions at physical light, strange and charm quark masses*, *Phys. Rev. D* **98** (2018) 054518 [1807.00495].

[4] [ETMC] A. Abdel-Rehim et al., *First physics results at the physical pion mass from $N_f = 2$ Wilson twisted mass fermions at maximal twist*, *Phys. Rev. D* **95** (2017) 094515 [1507.05068].

[5] [ALPHA] P. Dimopoulos, H. Simma and A. Vladikas, *Quenched B(K)-parameter from Osterwalder-Seiler tmQCD quarks and mass-splitting discretization effects*, *JHEP* **0907** (2009) 007 [0902.1074].

[6] D. Becirevic et al., *Exploring twisted mass lattice qcd with the clover term*, *Phys. Rev.* **D74** (2006) 034501 [hep-lat/0605006].

[7] Y. Iwasaki, *Renormalization Group Analysis of Lattice Theories and Improved Lattice Action: Two-Dimensional Nonlinear O(N) Sigma Model*, *Nucl.Phys.* **B258** (1985) 141.

[8] S. Aoki, R. Frezzotti and P. Weisz, *Computation of the improvement coefficient c(SW) to one loop with improved gluon actions*, *Nucl. Phys. B* **540** (1999) 501 [hep-lat/9808007].

[9] [ETMC] C. Alexandrou et al., *Ratio of kaon and pion leptonic decay constants with $N_f = 2 + 1 + 1$ Wilson-clover twisted-mass fermions*, 2104.06747.

[10] [ETMC] J. Finkenrath et al., *Twisted mass gauge ensembles at physical values of the light, strange and charm quark masses*, *PoS(LATTICE2021)284* (2021) .

[11] [FLAG] S. Aoki et al., *FLAG Review 2019: Flavour Lattice Averaging Group (FLAG)*, *Eur. Phys. J. C* **80** (2020) 113 [1902.08191].

[12] K. Osterwalder and E. Seiler, *Gauge Field Theories on the Lattice*, *Ann. Phys.* **110** (1978) 440.

[13] R. Frezzotti and G.C. Rossi, *Chirally improving Wilson fermions. II: Four-quark operators*, *JHEP* **10** (2004) 070 [hep-lat/0407002].

[14] [ETMC] C. Alexandrou et al., *Quark masses using twisted mass fermion gauge ensembles*, 2104.13408.

[15] [ETMC] B. Kostrzewa et al., *Gradient-flow scale setting with $N_f = 2 + 1 + 1$ Wilson-clover twisted-mass fermions*, *PoS(LATTICE2021)131* (2021) .

[16] [FLAG] S. Aoki et al., *Review of lattice results concerning low-energy particle physics*, *Eur. Phys. J. C* **77** (2017) 112 [1607.00299].

[17] M. Di Carlo, D. Giusti, V. Lubicz, G. Martinelli, C.T. Sachrajda, F. Sanfilippo et al., *Light-meson leptonic decay rates in lattice QCD+QED*, *Phys. Rev. D* **100** (2019) 034514 [1904.08731].

[18] R. Frezzotti, P.A. Grassi, S. Sint and P. Weisz, *Lattice QCD with a chirally twisted mass term*, *JHEP* **0108** (2001) 058 [hep-lat/0101001].

[19] [ETMC] M. Di Carlo et al., *Renormalization constants of quark bilinear operators in QCD with dynamical up, down, strange and charm quarks*, *PoS(LATTICE2021)399*.

[20] G. Colangelo, S. Durr and C. Haefeli, *Finite volume effects for meson masses and decay constants*, *Nucl. Phys. B* **721** (2005) 136 [hep-lat/0503014].

[21] J. Gasser, A. Rusetsky and I. Scimemi *Electromagnetic corrections in hadronic processes*, *Eur. Phys. J.* **C32** (2003) 97 [hep-ph/0305260 [hep-ph]].

[22] [ETMC] N. Carrasco et al., *Leptonic decay constants f_K, f_D, and f_{D_s} with $N_f = 2 + 1 + 1$ twisted-mass lattice QCD*, *Phys. Rev.* **D91** (2015) 054507 [1411.7908].

[23] Jülich Supercomputing Centre, *JURECA: Modular supercomputer at Jülich Supercomputing Centre*, *Journal of large-scale research facilities* **A132** (2018) 4.